Nanofiltration for Mixed Ion Systems with Commercial and Pore-Filled Membranes

Wayne W Jiang[a*], Jesus Garcia-Aleman[b], James M Dickson[b], and Ronald F Childs[a]

(Departments of [a]Chemistry and [b]Chemical Engineering, McMaster University, Hamilton, ON L8S 4M1Canada,
Tel : +1(905) 525-9140; Fax: +1(905)522-2509; E-mail: wenyi@chemistry.mcmaster.ca)

Abstract: Nanofiltration for mixed ion systems with commercial and pore-filled membranes was studied. A modified model was proposed based on the extended Nernst-Planck equation, Donnan equilibrium, and Gouy-Chapman theory. The performance of the commercial membrane (DDS HC50) was described successfully using this model. The model was also used to predict the performance of a pore-filled membrane. The model predicted the performance of the commercial membrane but failed to describe all the observed behavior of the pore-filled membrane. [Nature and Science, 2004,2(1):11-16].

Key words: modelling; extended Nernst-Planck equation, nanofiltration, mixed ion system

1 Introduction

Nanofiltration (NF) is a pressure driven membrane separation process where a solute is separated from a solution under pressure through a membrane. Nanofiltration membranes are considered to be "leaky" reverse osmosis (RO) membranes and nanofiltration is under lower pressure than reverse osmosis. NF membranes have intermediate molecular weight cut-off between reverse osmosis and ultrafiltration (UF) membranes (Petersen 1993). Nanofiltration has become an important process for various applications, including pulp processing (Peterson 1993), water purification, demineralization of whey in the dairy industry (van der Horst 1995), to concentrate organics (Perry 1989), and water softening (Mika 1999), etc.

Many researchers have investigated nanofiltration for salt separations in order to properly design and predict performance using mathematical models. When mixed solutes are present, the interaction between ions becomes large and is significantly influenced by Donnan equilibrium (Josson 1980, Nielson 1994, Tsuru 1991, Rios 1996, Mika 2001, Jiang 2003). The extended Nernst-Planck equation has been extensively used to model charged membranes (Dresner 1972, Josson 1980, Buck 1984, Tsuru 1991, and Petersen 1993). The basis and limitations of the extended Nernst-Planck equation applied to ionic transport in charged membranes have been discussed.

It has not been concluded whether high performance membranes for nanofiltration have porous heterogeneous or homogeneous structures. Mathematic models have been proposed to understand nanofiltration, such as a bundle of capillaries model (Wang 1995), the Hybrid Model (Bowen 1996 and 1997), etc. For example, Bowen *et al*. (1997) determined that activities inside membrane pores caused by solute-solute and solute-membrane ion interactions were accounted for by the effective charge density. This model contained three structural parameters: the effective membrane thickness, the effective charge density, and the membrane pore radius. The hindrance factors were related linearly to the ratio of solute to pore radius using finite element calculation (Bowen 1996 and 1997, Dean 1987). Using single electrolyte data, they were able to correlate the dependence of the effective charge density on the bulk concentration through a Freundlich type isotherm.

Josson (1980) successfully predicted negative rejections in reverse osmosis cellulose acetate membranes using the extended Nernst-Planck equation combined with a frictional and exclusion model. He assumed that Donnan equilibrium was valid through all the membrane thickness (Helfferich 1962). Recently, Nielson and Josson (1994) tried to introduce an analytical solution to the same problem. They were able to predict negative rejection in limiting cases based on bulk solution concentration. Rios (1996) established a mathematic model for the separation of Nafion membranes by simplifying the Nernst-Planck equation

by limiting to sufficiently high volume fluxes. Van der Horst (1995) solved the Nernst Planck equation as a difference equation. The accounted for concentration polarization due to the nature of solutes (whey permeate). Model predictions were in good agreement with the experimental data, but the parameters had limited physical significance.

In this study, the model of Josson (1994) is modified and compared to two sets of data, i.e., one is obtained from a commercial membrane (DDS HC50) and the other from a pore-filled cation-exchange membrane (Jiang 1999).

2 Model Derivations

The concentration profile across the membrane is obtained by rearranging Eq. 7 and using Eq. 2,

$$\frac{dC_{i,p}(x)}{dx}=\frac{J_V}{D_{i,\infty}E}\left(a_iC_{i,p}(x)-b_iC_i^p(x)\right)-\frac{z_iFC_{i,p}}{RT}\frac{d\Psi(x)}{dx} \quad (8)$$

Thus, the potential gradient is obtained as a function of the volume flux and ion concentrations,

$$\frac{d\Psi(x)}{dx}=\frac{RT}{FE}\cdot\frac{\sum\left(\frac{z_i}{D_{i,\infty}}\right)(a_iC_{i,p}(x)-b_iC_{i,p}^p}{\sum z^2C_{i,p}(x)}J_v \quad (9)$$

Eq. 9 is solved using the following boundary conditions, assuming (i) the concentration of species i in the feed is equal to that on the surface of membrane on the feed side ($x = 0$), Eq. 10, and (ii) the concentration of species i in the permeate is equal to that on the surface of membrane on the permeate side ($x = \lambda$),

$$C_{i,p}(0) = C_i^F \quad (10)$$

$$C_{i,p}(\lambda) = C_i^P \quad (11)$$

where λ is membrane thickness (m).

The concentrations at the interfaces between the membrane and feed/permeate solutions are calculated from Donnan equilibrium,

$$\frac{K_i}{K_{i,0}}=\left(\frac{C_{i,p}}{C_i}\right)\left(\frac{\gamma_{i,p}}{\gamma_i}\right)=\exp\left(-\frac{z_iF}{RT}\Delta\Psi_D\right) \quad (12)$$

where K_i, $K_{i,0}$, γ_i, and $\gamma_{i,p}$ are partition coefficient, zero partition coefficient, activity coefficient, and activity coefficient in membrane pores, respectively.

For (n) ions the model consists of (n - 1) coupled ODE that have to be solved numerically. The model has (3n + 2) parameters ($K_{i,0}$, b_i, a_i, X, λ/E) which account for membrane characteristics and solute-membrane interactions. The model was solved numerically using a variable order method for still/non-stiff ODE solver, and the parameters were estimated using a nonlinear least-squares routine (Levenberg-Marquardt).

For a dilute solution ($\gamma_i \approx \gamma_{i,p} \approx 1$), Eq. 8 can be modified to account for Donnan equilibrium, Eq. 12, throughout membrane cross section when pores are assumed to exist,

$$\frac{dC_{i,p}(x)}{dx}=\frac{J_v}{D_{i,\infty}E}\left(a_iC_{i,p}(x)-\frac{b_iC_i^pK_i^p}{K_i}\right)-\frac{z_iFC_{i,p}}{RT}\frac{d\Psi(x)}{d(x)} \quad (13)$$

and the electrical potential is given by

$$\frac{d\Psi(x)}{dx}=\frac{RT}{FR}\cdot\frac{\sum\left(\frac{z_i}{D_{i,\infty}}\right)\left(\frac{a_iC_{i,p}(x)}{K_i}-b_iC_i^pK_i^p\right)}{\sum z_i^2K_iC_i(x)}J_v \quad (14)$$

3 Experimental

The cation exchange membranes investigated in this study were a commercial reverse osmosis membrane and a pore-filled membrane. The commercial cation-exchange membrane is DDS HC50. The HC50 is a commercial membrane that consists of polyamide layer on a polysulfone support.

The pore-filled cation-exchange membrane was fabricated as described elsewhere (Jiang 1999). This pore-filled membrane consists of a polyethylene microfiltration substrate (pore size of 0.19 μm, thickness of 45 μm, and porosity of 78%) fabricated by the 3M Company (St. Paul, Minnesota, USA) and the polyelectrolytes, i.e., poly(styrene-sulfonic acid) groups. The pore-filled membrane used in this study had the following characteristics: 80% of mass gain of polystyrene, 2.5% of divinylbenzene, 67% of water content, and an ion-exchange capacity of 2.2 meq/g.

The pressure-driven experiments were carried out in a reverse osmosis/nanofiltration apparatus at 25°C (Jiang 2003). The solutes used were sodium chloride, sodium sulfate, magnesium chloride, and magnesium sulfate (Aldrich, analytical grade). The water used in

this study was deionzed water and carbon filtered. The concentrations of salts were measured using a Dionex ion chromatography, (Sunnyvale, California, USA).

4 Results and Discussion

This paper studied the nanofiltration performance predicted by the model developed above. The model was simplified by allowing the effective charges density to be accounted for by the zero partition coefficients. The following two sections describe the understanding of the membrane performance of separating mixed salts using an HC50 membrane and a pore-filled ion-exchange membrane.

5 Performance of HC50 Membrane

The water flux and an NaCl solution flux of the HC50 commercial membrane were measured. Fig. 1 shows the relationship between flux and pressure. It is not surprised to see that the linear relationships between the flux and the applied pressure. This is consistent with the findings of other researchers.

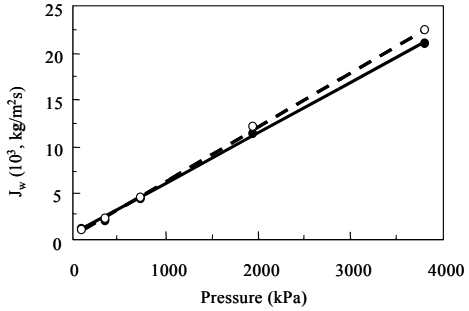

Fig.1 Flux versus applied pressure for water(dashed curve) and a 2 mol/m^3 of NaCl solution (solid curve)

The HC50 membrane was used in nanofiltration with a mixed salt solution system of $NaNO_3$ and Na_2SO_4. Fig. 2 shows the nanofiltration results for the commercial HC50 RO membrane. Fig. 2 is obtained by plotting the coion rejection versus the flux. The curves are the rejections predicted by the model proposed above. The data points are experimental data. Two different concentration ratios were used in the test, one marked as ▲ is 1:1 $NaNO_3$:Na_2SO_4 and the other as Δ is 1:10 $NaNO_3$:Na_2SO_4. As can be seen in Fig. 2, the model proposed above successfully predicted the performance of the commercial membranes, HC50.

The model predictions agree with the experimental nitrate rejection with great accuracy. The rejection greatly depends on the permeate flux. For example, the rejection of the more permeate ion (nitrate) decreases and of the less permeable ion (sulfate) increases as increasing the concentration of the less permeate ion (sulfate).

As can bee seen in Fig. 2, the model is able to predict a limiting rejection at infinite flux, and the minimum in nitrate rejection at low fluxes. The parameter estimated are given in Table 1. It can be inferred that Donnan exclusion (Kio's) dominates ion selectivity by the membrane. It is observed that the zero partition coefficient for the bivalent coion is several order of magnitude smaller that that for the monovalent coion and any counterion, which agrees with previous findings (Josson 1980). Steric effects are also shown to be important. At low flux, they are overpowered by Donnan exclusion mechanism. At higher flux, they have a greater contribution to solute transport. The values of the hindered diffusion and convection are relatively high compared to those obtained from the formulas of the ratio of solute to pore radius. But there is an agreement in that there is a greater correction in the dissuasive term than the convective term.

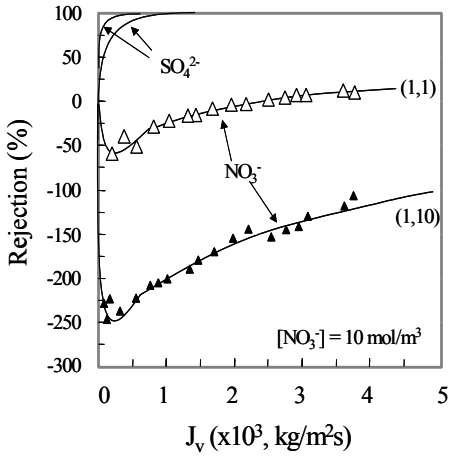

Fig. 2 Ion rejection versus permeate flux. The points (marked as ▲ and Δ) are experimental data and the curves are the model prediction. The nitrate concentration was kept constant (10 mol/m^3)

Table 1 Parameter estimates and 95% confidence intervals for membrane HC50 ($NaNO_3$ and Na_2SO_4)

Parameter	Numerical value	95% Confidence interval
K NO_3 0	0.52131	0.04364
K SO_4 0	0.00735	0.00052

K Na 0	0.30901	0.02123
b NO_3 0	2.41325	0.16892
b SO_4 0	73.5122	11.0268
b Na 0	5.21325	0.26066
a NO_3 0	0.91235	0.09123
a SO_4 0	0.84233	0.04211
a Na 0	0.89123	0.10694
λ/E(le4m)	0.27481	0.00311
Sum of square	0.33312	

The values obtained for the hindered diffusion and convection coefficients (Table 1) were used to back calculate a pore radius as described by Bowen *et al*.(1996 and 1997). The results is a pore radius of approximately 0.40 nm. With this we were able to compare the calculated value of the membrane effective thickness/water content with other authors. Bowen (1996) obtained an effective membrane thickness of 165 μm. They used a pore radius of 1 nm (mild steric effects) and set the porosity to unity. Taking into account that the characterization of the same membrane with a smaller pore radius would imply higher steric effects, and consequently the effective membrane thickness should be reasonably smaller (< 25 μm), in order to obtain the same performance.

6 Performance of Pore-filled Membrane

Fig. 3 shows the relationship between flux and pressure. A non-linear relationship was observed. This is consistent with the findings of other pore-filled membranes (Mika 1995, 1997, and 1999). However, this is not consistent with the data observed above for the commercial membrane. Another observation is that the pure water flux was lower than the solution flux. This is opposite to the results obtained for the commercial membrane. This is likely due to the change in conformation of polyelectrolytes in the pore-filled membrane with changing the pressure or ion strength. If this was true, the model should be modified accordingly.

The pore-filled membranes have a particular characteristics, especially the addition of an electrolyte leads to an increase in solution flux. This performance is inconsistent with that of commercial membranes where a higher feed concentration leads to a lower flux.

Polyelectrolytes play an important role in these processes. The higher flux is due to the interactions between the electrolyte solution and polyelectrolytes gels fixed in membrane pores. When pure water is used, the interactions between charged polyelectrolyte segments repel each other and the polyelectrolyte chains are forced to extend into the pores of the membranes. As the electrolyte concentration increases, the fixed charges are neutralized by the counterions, i.e., sodium ion, known as charge screening. Higher concentration of electrolyte leads to a greater internal pressure generated by the elastic springs in membrane pores. As a result, the balance results in a constant flux when the feed concentration is increased (Jiang 2003). If the concentration increases too high, the elastic springs may break. This may a possible explanation of the enhanced flux at high feed concentration.

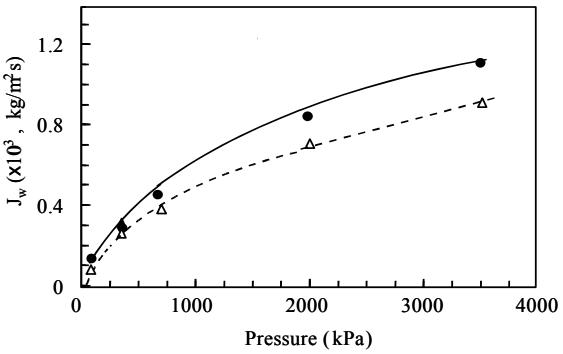

Fig. 3 Flux versus applied pressure for water (dashed curve) and a 2 mol/m^3 of NaCl solution (solid curve)

Fig. 4 shows the rejection as a function of permeate flux with two concentration ratios, i.e., [Na^+/Mg^{2+}] = 1:1 and 1:2. The points are the data of the experimental results and the curves are the model prediction. In both cases of two concentration ratios, the model was able to predict most of the data points for magnesium but could not predict the performance of sodium. It can be concluded that the model proposed here failed to predict consistently the performance of the pore-filled membranes, although the parameter estimates give a qualitative basis to analyze the behavior of this membrane. The parameter estimates used in the calculation are summarized in Table 2.

Donnan equilibrium plays an important roll in the separation of the pore-filled membrane. The parameter estimates show the same trend as the commercial membrane. Coions have smaller ratios of activities, and counterions have larger. Nevertheless, the values are much smaller in the pore-filled membrane which means that a greater charge in the membrane groups exists, thus a greater exclusion effect. For example, the zero

partition coefficient for sodium is three lower for the pore-filled than the commercial membrane.

(A) $[Na^+]$ = 1 mol/m^3 and $[Mg^{2+}]$ = 1 mol/m^3

(B) $[Na^+]$ = 1 mol/m^3 and $[Mg^{2+}]$ = 2 mol/m^3.

The model proposed in this work, as well as the models mentioned in Introduction under several assumptions. First, the solution flux should decrease with increasing feed concentration (osmotic pressure) since it is a function of the intrinsic permeability of the membrane (constant) and the effective pressure. The model cannot possibly predict higher values of J_v with increasing bulk concentration as no charge screening effect is included.

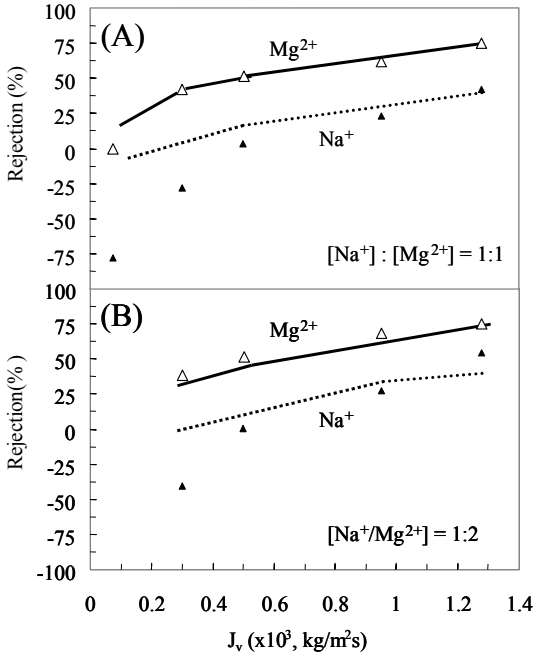

Fig. 4 Ion rejection as a function of permeate flux. The dotted and solid curves are model predictions for magnesium and sodium, respectively, and points are experimental data

Table 2 Parameter estimates and 95% confidence intervals for pore-filled membrane (NaCl:$MgCl_2$)

Parameter	Numerical value	95% Confidence interval
K Na 0	0.10020	0.103
K Mg 0	0.45162	0.377
K Cl 0	0.10218	0.974
b Na 0	7.98953	10.32
b Mg 0	10.3928	19.48
b Cl 0	1.00005	1.826
a Na 0	0.57266	0.688
a Mg 0	0.61570	0.688
a Cl 0	0.57767	1.127
λ/E(le4m)	12.8645	12.56
Sum of square	0.98541	

Second, the structural properties of the membrane parameters are considered to be constant, ie., thickness, water content, pore size, gel structure, etc. However, it was found that the parameters of pore-filled membranes may change as changing conditions such as pressure, ion strength, pH, etc., due to the nature of polylectrolytes (Mika 1995, 1997, 1999 and Jiang 2003).

Third, the steric hindrance coefficients do not depend on pressure or solute concentration. Using the explanation for charge screening and a correlation from Table 1, the friction parameters should decrease as the pore radius increases, i.e., as ion concentration increase in the pore-filled membrane. The crosslinking of the polyelectrolyte protects the pore-filling from total collapse due to charge screening and then the flux stays constant at the higher concentrations. Nevertheless, it is evident that model fits the data properly at high fluxes.

7 Conclusion

The performance of a commercial membrane was described successfully using a modified model based on the extended Nernst-Planck equation and Donnan exclusion. The model showed agreement with results obtained by other authors. The model also was used to predict the performance of a pore-filled membranes. In this case there was insufficient data to fit the model well and the model could not describe all the observed behavior.

However, new directions to extend the membrane modeling to such phenomena are suggested. There has to be developed an effective mean to account charge screening since this interaction not only dynamically affects the pore radius and hence steric but also has an effect on the effective charge density distribution and ion partition into the membrane.

The authors acknowledge the financial support from the Natural Sciences and Engineering Research Council of Canada and the Science and Technology National Council of Mexico. Data of this work were presented at the International Conference on Membranes and Membrane Processes, Toronto, Ontario, Canada (May 1999).

Symbols

a : hindered convection parameter
b_i : hindered diffusion parameter
C_i : ion concentration in solution, mol/m^3
$C_{i,p}(x)$: ion concentration in pore at point x, mol/m^3
C_X : membrane volumetric charge density, mol/m^3
D_i : ionic diffusivity inside the pore, m^2/s
$D_{i,4}$: ionic diffusivity at infinite dilution, m^2/s
E : electric potential, V
F : Faraday's constant, 9,6487.0 C/mol
I : electrical current, C/s
J_i : ion flux based on membrane area, mol/m^2 s
J_v : volumetric solution flux, m^3/m^2 s
K_i : partition coefficient, dimensionless
$K_{i,0}$: zero partition coefficient, dimensionless
m : molality, mol/kg
n : total number of ions, dimensionless
R : universal gas constant, 8.314 J/mol K
T : absolute temperature, K
x : axial coordinate, m
z_i : ion valence, dimensionless
$,$: membrane porosity dimensionless
8 : effective thickness of the membrane, m
Θ : membrane electrical potential, V
T : sign of the charge density of membrane

Corresponding to (Current address):

Wayne Jiang
National Food Safety and Toxicology Center
Michigan State University
East Lansing, Michigan 48824-1302, USA
Telephone: 517-432-3100
Fax: 517-432-2310
E-mail: jiangw@cvm.msu.edu

References

[1] Bowen WR, Mohammad, AW Hilal N. Characterisation of nanofiltration membranes for predictive purposes – Use of salt, uncharged solutes and atomic force microscopy. J Membrane Sci , 1997,126:91-105.

[2] Bowen WR, Mukhtar H. Characterisation and prediction of separation performance of nanofiltration membranes. J Membrane Sci , 1996,112: 263-74.

[3] Buck RP. Kinetics of bulk and interfacial ionic motion: Microscopic bases and limits for the Nernst-Planck equation applied to membrane systems. J Membrane Sci , 1984 ,17:51-62.

[4] Cussler EL. Diffusion: Mass Transfer in Fluid System, Cambridge University Press, Cambridge, UK , 1985.

[5] Deen WM. Hindered transport of large molecules in liquid-filled pores. AIChE J , 1987;33(9):1409-25.

[6] Dresner L. Stability of the extended Nernst-Plank equations in the description of hyperfiltration through ion-exchange membranes. J Physical Chem , 1982;76(6):16.

[7] Helfferich H. Ion Exchange, McGraw-Hill, New York, New York , 1962.

[8] Jiang W. Preparation and characterization of pore-filled cation-exchange membranes, Ph.D. Thesis, McMaster University, Hamilton, Ontario , 1999.

[9] Jiang W, Childs RF, Mika AM, Dickson JM, Pore-filled cation-exchange membranes containing poly(styrene-sulfonic acid) gels. Desalination , 2003 , 159:253-66.

[10] Jiang W, Childs RF, Mika AM, Dickson JM. Pore-filled membranes capable of selective negative rejections. Science and Nature., 2003 , 1(1) 21-6.

[11] Josson G. Coupling of ion fluxes by boundary-, diffusion- and streaming- potentials under reverse osmosis conditions, Proceedings of the 7th. International Symposium on Fresh Water from the Sea , 1980 , 2: 153.

[12] Mika AM, Childs RF, Dickson JM, McCarry BE, Gagnon DR. A new class of polyelectrolyte-filled microfiltration membranes with environmentally controlled porosity. J Membrane Sci , 1995 , 108:37-56.

[13] Mika AM, Childs RF, West M, Lott JNA, Poly(4-vinylpyridine)-filled microfiltration membranes: Physicochemical properties and morphology. J Membrane Sci , 1997;136:221-32.

[14] Mika AM, Childs RF, Dickson JM. Ultra-low pressure water softening: a new approach to membrane construction. Desalination, 1999;121:149-58.

[15] Mika AM, Pandey AK, Childs RF. Ultra-low-pressure water softening with pore-filled membranes. Desalination 2001;140:265-75.

[16] Mika AM, Childs RF, Dickson JM. Salt separation and hydrodynamic permeability of porous membrane filled with pH-sensitive gel. J Membrane Sci 2002;206:19-30.

[17] Nielsen DW, Josson G. Bulk-phase criteria for negative ion rejection in nanofiltration of multicomponent salt solutions. Sep. Sci. and Tech 1994;29(9):1165-82.

[18] Perry M, Linder C. Intermediate reverse osmosis ultrafiltration membranes for concentration and desalting of low molecular weight organic solutions. Desalination 1989;71:223-45.

[19] Petersen RJ. Composite reverse osmosis and nanofiltration membranes. J Membrane Sci 1993;83:81-95 (1993).

[20] Rios GM, Joulie R, Sarrade SJ, Carles M. Investigation of ion separation by microporous nanofiltration membranes. AIChE J 1996; 42(9):2521-2528.

[21] Sourirajan S. Reverse Osmosis, Academic Press, New York. 1970.

[22] Tsuru T, Nakao S, Kimura S. Calculation of ion rejection by extended Nernst-Plank equation with charged reverse osmosis membranes for single and mixed electrolyte solutions. J Chem Eng Japan 1991;24(4):511-7.

[23] Tsuru T, Urairi M, Nakao S, Kimura S. Reverse osmosis of single and mixed electrolytes with charged membranes:

Experiment and analysis, J. Chem. Eng. Japan 1991;24(4):518-524.

[24] Van der Horst HC, Timmer JMK, Leeders RJ. Use of Nanofiltration for concentration and demineralization in the dairy industry: Model for mass transport. J Membrane Sci 1995;104:205-217.

[25] Wang X, Tsuru T, Nakao S, and Kimura S. Electrolyte transport through nanofiltration membranes by the space-charged model and the comparison with Teorell-Myer-Sievers model. J Membrane Sci 1995;103:117-33.

[26] Wang X, Tsuru T, Togoh M, Nakao S, Kimura S. Evaluation of pore structure and electrical properties of nanofiltration membranes. J Chem Eng Japan 1995;28(2):168-92.